



Functional pathways associated with human carotid atheroma: a proteomics analysis

Ali Nehme^{1,2} · Firas Kobeissy³ · Jingfu Zhao⁴ · Rui Zhu⁴ · Patrick Feugier⁵ · Yehia Mechref⁴ · Kazem Zibara^{2,6}

Received: 6 May 2018 / Revised: 24 July 2018 / Accepted: 14 August 2018 / Published online: 7 January 2019
© The Japanese Society of Hypertension 2019

Abstract

Advances in large-scale analysis are becoming very useful in understanding health and disease. Here, we used high-throughput mass spectrometry to identify differentially expressed proteins between early and advanced lesions. Carotid endarterectomy samples were collected and dissected into early and advanced atherosclerotic lesion portions. Proteins were extracted and subjected to liquid chromatography–tandem mass spectrometry (LC–MS/MS) analysis. Differentially expressed proteins were identified and verified using multiple reaction monitoring (MRM), on which advanced systems biology and enrichment analyses were performed. The identified proteins were further compared to the transcriptomic data of 32 paired samples obtained from early and advanced atherosclerotic lesions. A total of 95 proteins were upregulated, and 117 proteins were downregulated in advanced lesions compared to early atherosclerotic lesions ($p < 0.05$). The upregulated proteins were associated with proatherogenic processes, whereas downregulated proteins were involved in extracellular matrix organization and vascular smooth muscle cytoskeleton. Many of the identified proteins were linked to various “upstream regulators”, among which TGF β had the highest connections. Specifically, a total of 19 genes were commonly upregulated, and 30 genes were downregulated at the mRNA and protein levels. These genes were involved in vascular smooth muscle cell activity, for which enriched transcription factors were identified. This study deciphers altered pathways in atherosclerosis and identifies upstream regulators that could be candidate targets for treatment.

Keywords Atherosclerosis · Carotid artery · Proteome · Transcriptome · Transcription regulators

These authors contributed equally: Ali Nehme, Firas Kobeissy

Supplementary information The online version of this article (<https://doi.org/10.1038/s41440-018-0192-4>) contains supplementary material, which is available to authorized users.

✉ Yehia Mechref
yehia.mechref@ttu.edu

✉ Kazem Zibara
kzibara@ul.edu.lb

¹ EA4173, Functional genomics of arterial hypertension, UCBL-1, Villeurbanne, France

² PRASE, DSST, Lebanese University, Beirut, Lebanon

³ Department of Biochemistry and Molecular Genetics, Faculty of Medicine, American University of Beirut, Beirut, Lebanon

⁴ Department of Chemistry and Biochemistry, Texas Tech University, Lubbock, Texas 79409, USA

⁵ Service de Chirurgie Vasculaire, Hôpital Universitaire E Herriot, Lyon 69008, France

⁶ Department of Biology, Faculty of Sciences-I, Lebanese University, Beirut, Lebanon

Introduction

Atherosclerosis is the main cause of ischemic heart disease and stroke, which have been the major causes of death during the past decade [1]. Atherosclerosis develops as a result of the combinatorial effects of more than 300 risk factors, including smoking, metabolic syndrome, hypertension, and diabetes. These factors lead to the initiation of local atherogenic processes in the vessel wall that result in the formation of an atherosclerotic plaque, leading to cardiovascular complications and death [2].

According to the “response-to-injury” hypothesis, inflammation is the key contributor to all stages of atherosclerosis, from initial lesions to plaque rupture [3]. Initially, external risk factors cause vascular wall injury, mainly endothelial dysfunction and lipid accumulation [4]. This injury leads to the recruitment of macrophages and vascular smooth muscle cells (VSMCs) to the site of injury that will differentiate, proliferate, engulf accumulating lipids, and secrete cytokines and proinflammatory factors. The latter

factors result in a local non-resolving inflammatory condition that progresses into atherosclerotic lesion growth [3].

Advancements in systems biology and large-scale analysis are becoming very useful in deciphering new proteins involved in health and disease [5]. Several studies have been performed to identify the molecular pathways implicated in disease initiation and development. However, changes at the RNA level may not reflect the true functional aspect that is defined by the protein arsenal of a cell. Hence, the quantification and characterization of cellular proteins is of extreme significance in order to understand molecular processes that mediate cellular functions. Recently, the development of new proteomics tools, such as high-throughput mass spectrometry, is improving our understanding of diseases by accelerating the discovery of new candidate targets and revealing the functional pathways within a tissue or a disease.

In this study, we used liquid chromatography–tandem mass spectrometry (LC–MS/MS) to reveal the proteomes of human carotid atherosclerotic plaques in early and advanced lesions. Differentially expressed proteins were further validated by multiple reaction monitoring (MRM) and were compared to transcriptomic microarray data. Our results showed that most of the altered proteins were involved in local inflammatory reactions, tissue remodeling and thrombosis. In addition, we revealed novel candidate regulators that interact with and are implicated in the expression of multiple proteins that are altered between early and advanced lesions.

Materials and methods

Sample collection and preparation

This study conforms to the principles outlined in the declaration of Helsinki [6]. All procedures were approved by the local ethical committee (ethical approval number SC090966), and patients gave informed consent prior to the use of their samples. A total of 6 carotid endarterectomy samples were collected from the Edouard Herriot hospital in Lyon (France). Patients were between 58 and 88 years old. The samples were dissected within 2 h after operation, and each was divided into two portions: atheroma plaque (ATH), corresponding to atherosclerotic lesions with Stary stage ≥ 4 , and macroscopically intact tissue (MIT), with Stary stage ≤ 2 [7]. No exclusion criteria were used for sample selection.

Protein extraction and digestion

Carotid tissue samples (30–100 mg) were washed with 50 mM ABC buffer to remove blood. A bead beating

homogenizer (Beadbug microtube homogenizer, Benchmark Scientific, Edison, NJ) was applied to perform cell lysis. Tissues were mixed with 5% sodium deoxycholate (SDC) (Sigma-Aldrich, St. Louis, MO) solution and 3 mm zirconium beads (OPS Diagnostics, Lebanon, NJ) in a 2-mL microtube. The solution of 5% SDC was added for efficient protein extraction. The samples were homogenized at 4 °C at 4000 rpm for 30 s, followed by a 30-s pause. This step was repeated six times. Next, the tissue lysate was sonicated for 30 min in a 0 °C ice-water bath to enhance protein dissolution. After centrifuging at 21,100 $\times g$ for 10 min, the supernatant was collected and diluted 10 times by adding 50 mM ammonium bicarbonate (ABC) buffer. The protein concentration was determined using a BCA protein assay kit (Thermo Scientific/Pierce, Rockford, IL) following the manufacturer's instruction.

A 15- μg aliquot of extracted proteins from each sample was then subjected to reduction, alkylation and tryptic digestion. An ABC (50 mM)-SDC (0.5%) solution was first added to the samples to maintain a volume of 50 μL . Proteins were thermally denatured at 80 °C for 10 min. The reduction of proteins was performed by adding a 1.25- μL aliquot of 200 mM dithiothreitol (DTT) solution and incubating at 60 °C for 45 min. The reduced proteins were then alkylated by adding a 5- μL aliquot of 200 mM iodoacetamide (IAA) solution and incubating at 37 °C in the dark for 45 min. To quench the excessive IAA, a 1.25- μL aliquot of DTT solution was added again, and the samples were incubated at 37 °C for 30 min. Following the reduction and alkylation of proteins, trypsin (Promega, Madison, WI) was added at a ratio of 1:25 (enzyme: proteins, w/w) into samples, which were then incubated at 37 °C for 18 h. After incubation, formic acid was added at a final concentration of 0.5% (v/v) for the purposes of both quenching the enzymatic reaction and removing the SDC detergent. Samples were then mixed thoroughly and centrifuged at 21,100 $\times g$ for 10 min. The supernatant was collected, speed-vac dried and resuspended in aqueous solution containing 2% acetonitrile (ACN) and 0.1% formic acid (FA) prior to LC–MS/MS analysis.

LC–MS/MS measurement

One microgram aliquots of tryptic digests were subjected to untargeted proteomic analysis. A Dionex 3000 Ultimate nano-LC (Dionex, Sunnyvale, CA) interfaced to an LTQ Orbitrap Velos mass spectrometer (Thermo Scientific, San Jose, CA) equipped with an ESI source was used for the analysis. Tryptic digests were first loaded to an Acclaim PepMap100 C18 guard column (3 μm , 100 Å, Dionex) at a flow rate of 3 $\mu L/min$ for online desalting. Next, the peptide separation was achieved using an Acclaim PepMap100 C18 capillary column (75 μm id \times 150 mm, 2 μm , 100 Å, Dionex) at

0.35 $\mu\text{L}/\text{min}$ for 120 min. The mobile phase A contained 2% ACN, 0.1% FA and 97.9% water, while mobile phase B contained 0.1% formic acid in ACN. The LC gradient was as follows: Solvent B was kept at 5% for the first 10 min and was increased from 5 to 20% over 55 min, 20–30% over 25 min, 30–50% over 20 min, 50%–80% over 1 min, kept at 80% for 4 min, decreased from 80 to 5% over 1 min and finally maintained at 5% over 4 min.

The LTQ Orbitrap Velos was used in data-dependent acquisition mode. The scan events were set as a full MS scan of m/z 400–2000 at a mass resolution of 15,000, followed by CID MS/MS scan repeated on the 10 most intense ions selected from the previous full MS scan with an isolation window of m/z 3.0. The normalized collision energy was set to 35% with an activation Q value of 0.25 and an activation time of 10 ms. Dynamic exclusion was enabled with a repeat count of 2, a repeat duration of 30 s and an exclusion duration of 90 s.

MRM experiment was further performed to confirm untargeted quantitative analysis of the results. The LC gradient described in the untargeted analysis was also used for the MRM experiment, in which a TSQ Vantage mass spectrometer was employed (Thermo Scientific, San Jose, CA). The transition list was generated using Pinpoint (Thermo Scientific), as previously described [8]. In total, 270 transitions of 90 peptides for 53 proteins were monitored in the MRM experiment. Aliquots of peptides (A 1.5- μg aliquot of each) were subjected to LC–MRM–MS analysis. The TSQ Vantage mass spectrometer was operated in positive mode. Peptides were introduced into the TSQ Vantage via the ESI source at a voltage of 1800 V. The chromatogram filter peak width was set to 10.0 s, and the collision gas pressure was set to 1.5 mTorr. In the SRM setting, the Q1 peak width (full width at half maximum) was 0.70 Da, and the cycle time was 6.0 s. The collision energy (CE) for each targeted peptide is predicted by Pinpoint according to the following equations: $\text{CE}(+2) = 0.034 \times m/z + 3.314(\text{eV})$, $\text{CE}(+3) = 0.044 \times m/z + 3.314(\text{eV})$. The maximum CE was 60 eV.

LC–MS/MS data analysis

For untargeted LC–MS/MS data, the raw files were converted to mascot generic format (*.mgf) files using Proteome Discover version 1.2 (Thermo Scientific, San Jose, CA). The *.mgf files were subjected to MASCOT version 2.4 (Matrix Science Inc., Boston, MA) to search against the UniProt database (Homo sapiens, 20214 entries) for identification. Carbamidomethylation of cysteine was defined as a fixed modification and oxidation of methionine as a variable modification. In database searching, peptides were matched with a tolerance of 10 ppm for precursors and 0.8 Da for CID MS/MS fragments. The enzyme was specified

as trypsin, and a maximum of 2 mis-cleavages was allowed. The results acquired from MASCOT searching were then uploaded to Scaffold (version 3.6.3, Proteome Software, Portland, OR) for verification and quantification. Only identifications with a minimum peptide threshold of 95%, a minimum protein threshold of 99% and at least 2 identified peptides were qualified for quantitation.

All raw files acquired from the MRM experiment were imported into Pinpoint to perform quantitative analysis. The quantitation of the LC–MRM–MS analysis was based on peak areas. The protein abundance was measured by summing up peak areas of all the corresponding transitions. Peak areas were averaged using replicates for the comparison between groups. Proteins with >1.5-fold changes in upregulation/downregulation for all the 6 samples and false discovery rate (FDR) < 0.05 were considered as significantly altered. Given that the mass spectrometric quantification is usually associated with 20% RSD, a consensus conservative threshold of 1.5-fold was applied [9].

Transcriptomic data analysis

To identify regulated proteins, differentially expressed proteins were analyzed against transcriptomic data. The GSE43292 dataset available on the GEO database, which contains previously studied paired MIT and ATH samples from 32 patients, was analyzed using the GEO2R web-tool to extract differentially expressed genes. Representative probe sets with the highest mean expression across all samples were retained for further analysis. Genes with false discovery rate (FDR)-adjusted p -value < 0.01 and >1.5-fold change were considered as significantly altered. The resulting genes were then compared to the differentially expressed proteins using the InteractiVenn web tool [10] to extract commonly altered genes and proteins, which were further subjected to enrichment analysis using PANTHER and Enrichr web-based tools.

Bioinformatics, subnetwork enrichment pathway analyses and statistical testing

Principle component analysis (PCA) and hierarchical clustering were applied on samples based on the expression of significantly altered proteins [11]. Upregulated and downregulated proteins were separately evaluated for enriched biological processes, molecular functions and pathways using the Protein ANalysis THrough Evolutionary Relationships (PANTHER) classification system [12]. In addition, enrichment analysis was also performed using “Enrichr” [13], a web-based tool that identifies transcription factors potentially associated with a set of genes based on robust statistical calculations. Elsevier’s Pathway Studio version 9.0 (Ariadne Genomics/Elsevier) was used to

deduce relationships among upregulated proteins using the Ariadne ResNet database [14, 15]. The “Subnetwork Enrichment Analysis” (SNEA) algorithm was selected to extract statistically significant altered biological and functional pathways relating to the set of proteins. In our analysis, “GenBank” ID and gene symbols from each set were imported to the software to form an experimental dataset. For the reconstruction of networks of pathways, biological processes and molecular functions were evaluated for each single protein hit and its associated targets (networks and pathways). Moreover, the differentially upregulated and downregulated proteins were analyzed using Ingenuity® Pathway Analysis (IPA®, QIAGEN Redwood City, USA), a software program that enables the identification of biological pathways and functions based on a particular dataset of proteins [16]. Significantly altered proteins ($p < 0.05$) with greater than twofold change between early and advanced lesions were analyzed using the Ingenuity Knowledge Base for their experimentally observed and predicted interactions (high confidence) in endothelial cells, vascular smooth muscle cells, and inflammatory cells of human, mouse and rat.

Results

Significantly altered proteins

Of the 621 measured proteins, 215 had a significant >1.5-fold modulation between the 2 tissues (Supplementary Table 1). A total of 95 proteins showed increased expression in advanced lesions (ATH), of which 8 proteins were not expressed in MIT (Supplementary Table 1). Additionally, 15 of the 120 downregulated proteins (1.5-fold change) were expressed in MIT, but not in atheroma (Supplementary Table 2). The expression levels of the identified proteins were then used to construct gene dendrograms using hierarchical clustering (Fig. 1) and PCA (data not shown), which clearly discriminated MIT from ATH samples.

The top 50 proteins, upregulated and downregulated, with the highest fold changes were validated by MRM (Fig. 2a and Supplementary Figure 1). All measured proteins showed consistent upregulation/downregulation results in MRM, compared to untargeted analysis, except for AP2B1, ARPC2, and AT2B4 (Fig. 2b).

Gene ontology and functional networks associated with differentially expressed proteins

To further understand the roles of the altered proteins at the cellular level, analysis of upregulated and downregulated proteins was performed using the PANTHER classification system. Interestingly, upregulated proteins were associated

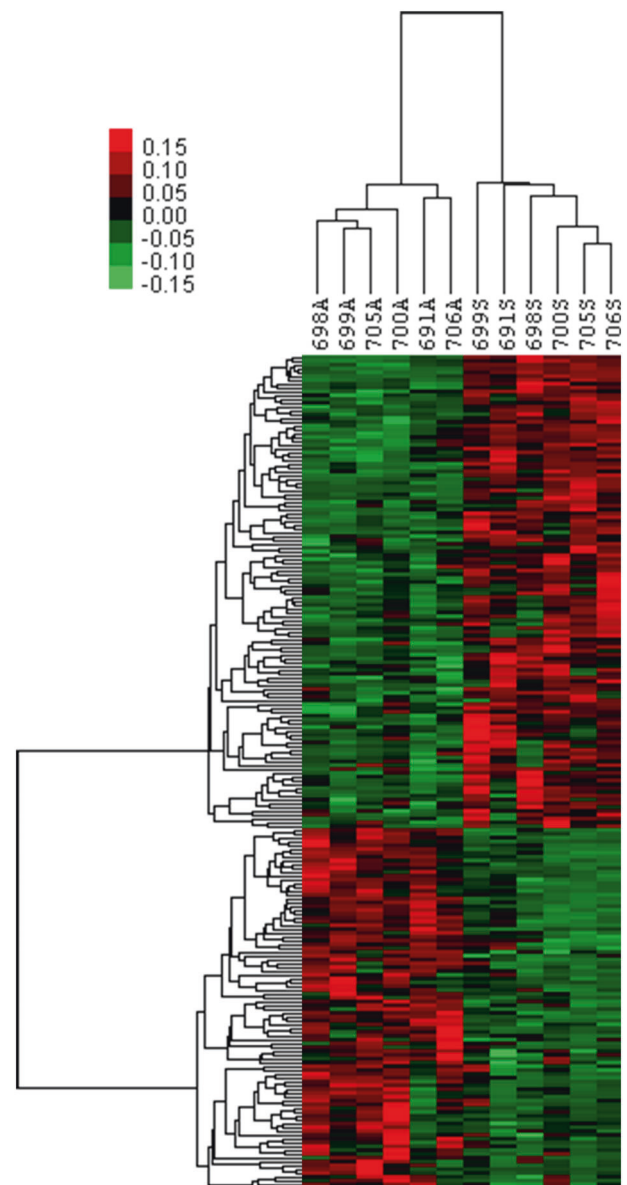


Fig. 1 Heat map representation of the differentially expressed proteins. Hierarchical clustering analysis of protein expression profiles was performed using Cluster 3.0 software (<http://bonsai.hgc.jp>). The heat map was created using non-logged expression profiles, with centered and normalized genes and arrays. MIT samples were designated by S; whereas, ATH samples were designated by A. Numbers next to the data points indicate the replicate numbers

with multiple proatherogenic functions related to immune, cellular and metabolic processes, such as lipid transport, macrophage activation, cell-mediated immune response, blood coagulation, cellular adhesion, growth, and survival (Fig. 3a and Supplementary Table 3). In contrast, downregulated proteins were related to tissue remodeling, mainly VSMC cytoskeletal proteins and extracellular matrix (ECM) components (Fig. 3b and Supplementary Table 4).

The upregulated proteins were then analyzed using Pathway Studio for biological functions, and a subcellular

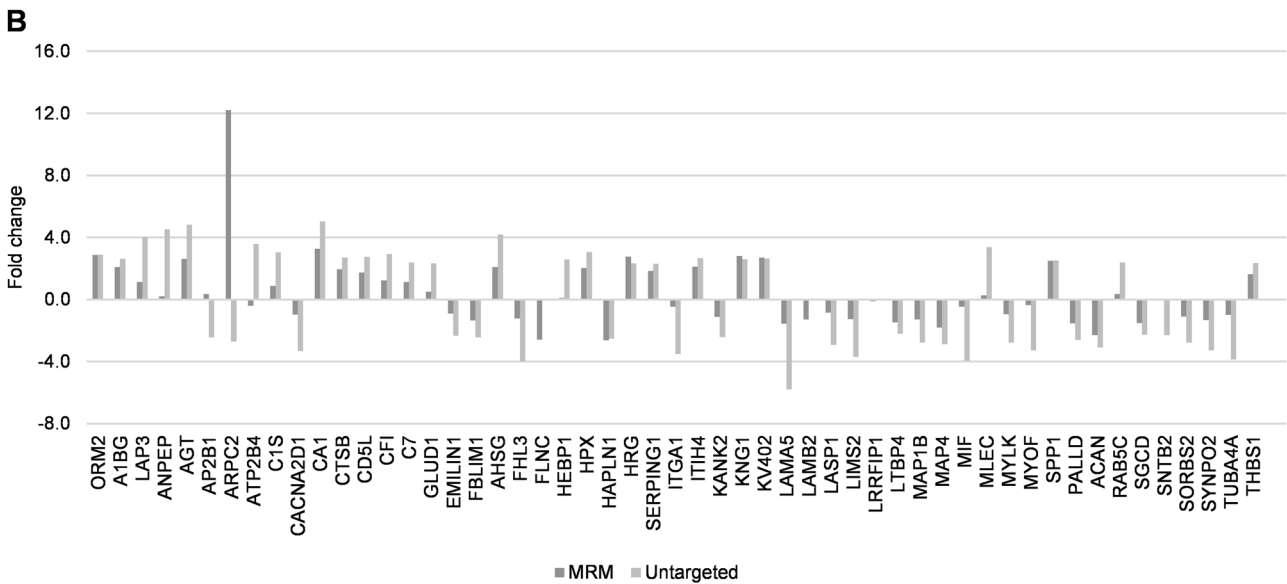
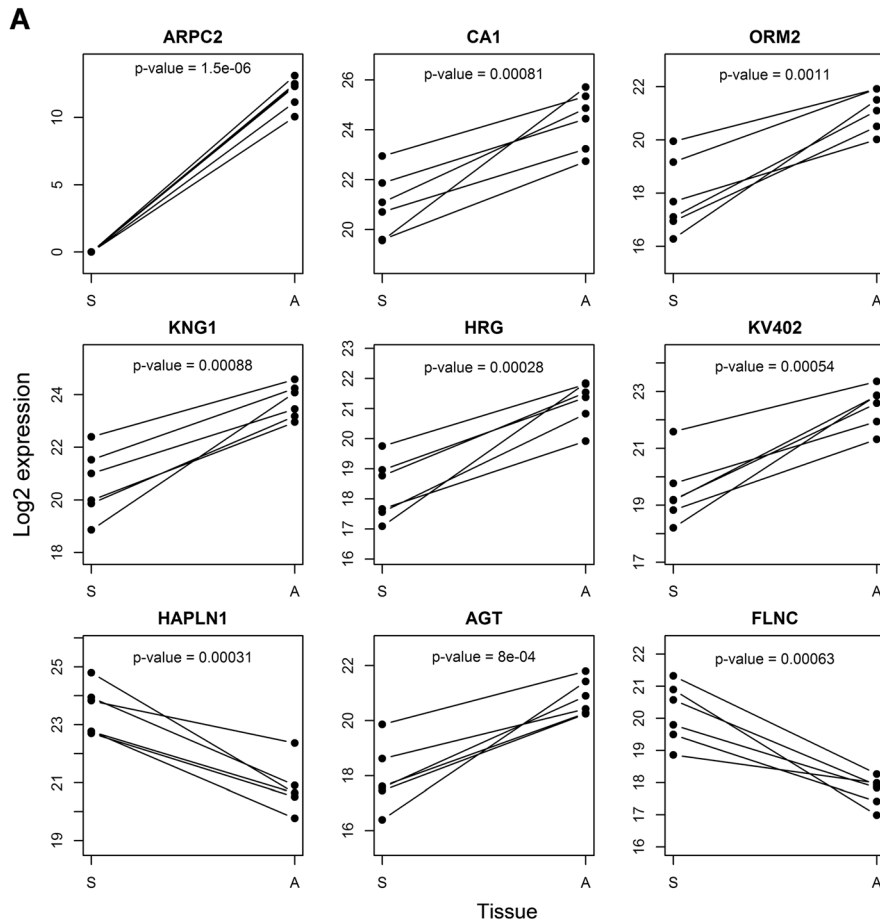


Fig. 2 Validation by multiple reaction monitoring (MRM). **a** Top upregulated and downregulated proteins with highest fold changes (FCs) between early and advanced lesions, measured by MRM. **b**

Comparison of FCs between untargeted and MRM results. AP2B1, ARPC2, and ATP2B4 were removed from the plot. S macroscopically intact tissue; A advanced atheroma lesion

network was constructed. The network revealed that upregulated proteins from different cellular compartments were associated with atherosclerosis and several pro-atherogenic

processes, including lipid transport, inflammation, VSMC proliferation, oxidative stress, cell movement, necrosis, and thrombosis (Fig. 4).

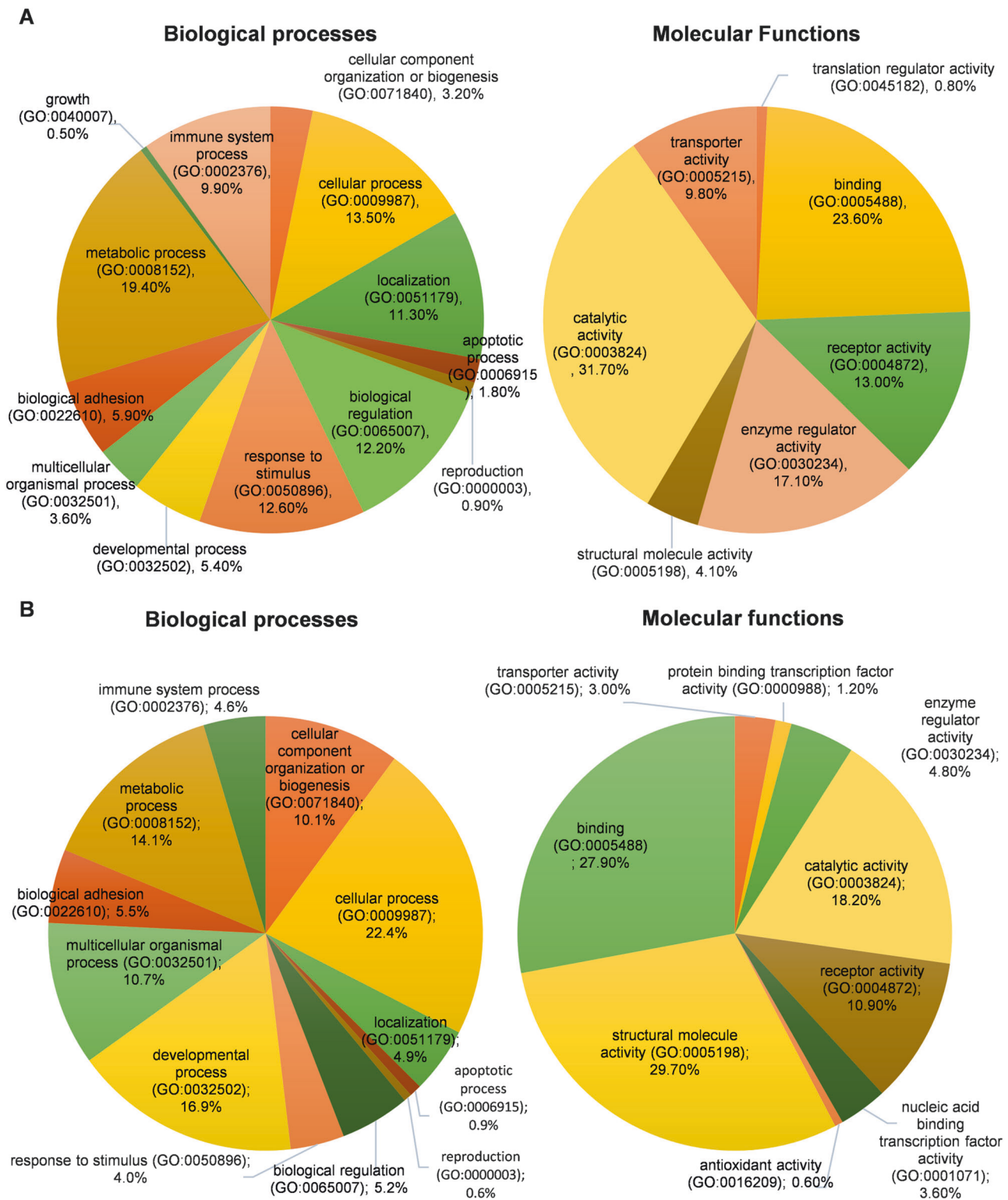


Fig. 3 Gene ontology associated with differentially expressed proteins. **a** Biological processes (left) and molecular functions (right) related to upregulated proteins in advanced compared to early lesions.

b Biological processes (left) and molecular functions (right) related to downregulated proteins in advanced compared to early lesions

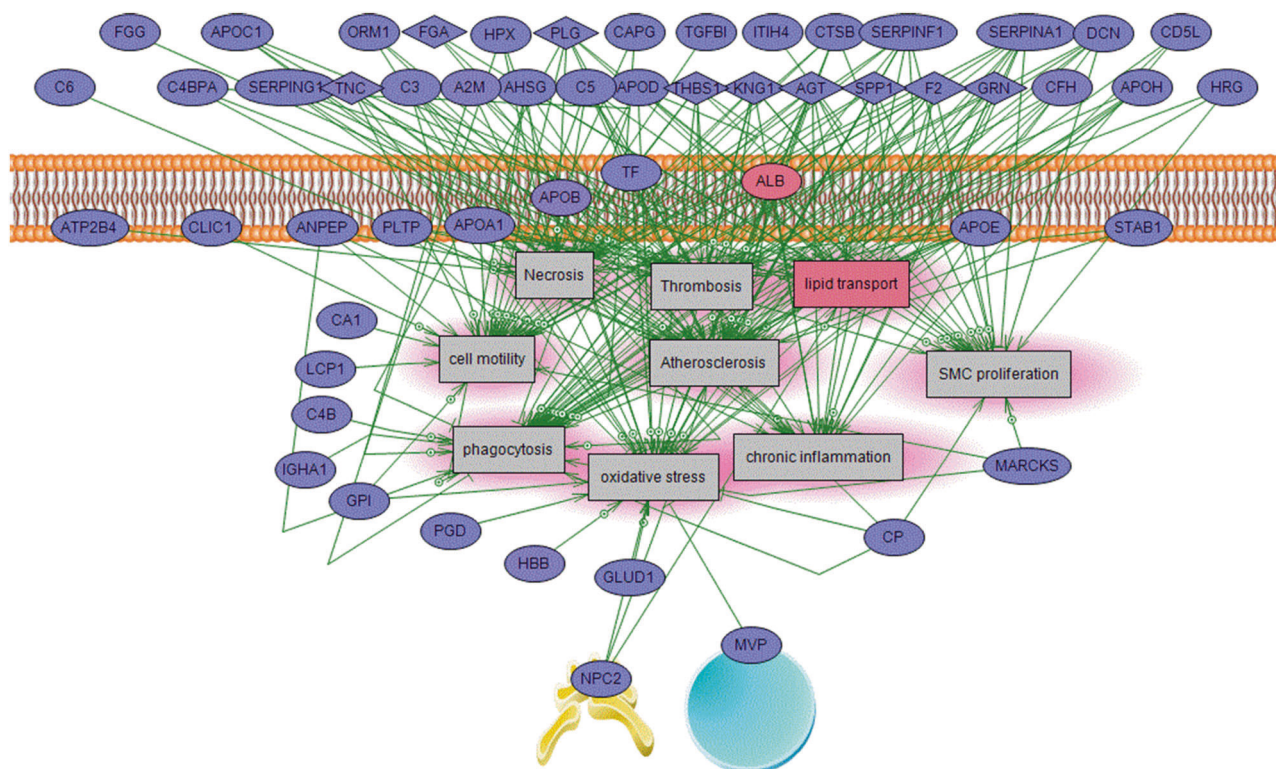


Fig. 4 Biological pathways associated with upregulated proteins during atherosclerotic lesion progression

Subcellular networks and candidate upstream regulators

To reveal the subcellular networks associated with the differentially expressed proteins, pathway enrichment analysis was performed using the IPA platform based on specific criteria (see Materials and Methods section). Network analysis resulted in the identification of different biological pathways, including acute phase response signaling, LXR/RXR and FXR/RXR activation, complement system, junctional signaling and cytoskeletal signaling (Table 1, Supplementary Figures 2 & 3).

In addition to subcellular networks, IPA was used to identify candidate upstream regulators that are directly or indirectly involved in the expression of the identified differentially altered proteins (Table 2). The master regulator p53 (Tp53), which can regulate the expression of a large number of the identified differentially expressed proteins, was found at the top of the candidate regulators list. Other regulators, such as MYC, which controls the expression of other proteins within the array, were also observed (Supplementary Figure 4). Interestingly, global network analysis showed that the identified proteins were highly connected to other proteins known to play central roles in atherosclerotic lesion development and progression, including TGFBI, ERK1, MAPK, MEK, JNK, PDGF, and TNF (Supplementary Figure 5).

Genes commonly altered at the mRNA and protein levels

A total of 535 upregulated and 389 downregulated genes were extracted from the GSE43292 dataset, containing 32 paired early and advanced atherosclerotic lesions, based on the statistical criteria mentioned in the Materials and Methods section. Comparison between differentially expressed genes and proteins showed that totals of 19 and 30 genes were commonly upregulated and downregulated, respectively, at the mRNA and protein levels (Supplementary Figure 6). Interestingly, upregulated genes were associated with complement activation, whereas downregulated genes were related to cytoskeletal organization associated with the contractile apparatus of VSMCs (Supplementary Table 6). The identified genes were further analyzed using “Enrichr” software to identify potential TFs associated with the extracted genes. Interestingly, a set of the upregulated genes was experimentally linked to NR1H3 in atherosclerotic foam cells, and some had their promoter sequences enriched in binding sites for FOXJ1, SND1, and NFKB1 (Supplementary Table 7). Furthermore, ChIP enrichment analysis (CHEA) identified multiple TFs that are highly associated with the downregulated genes in different cell lines (Supplementary Table 8). In addition, their promoters were enriched in binding sites for SRF, JUN, RUNX1, and HINFP (Supplementary Table 8).

Table 1 Top canonical pathways extracted using Ingenuity Pathway Analysis

Ingenuity canonical pathways	-log p-value	z-score	Involved proteins
Acute phase response signaling	2.66E+01	2.31	SERPINF1, APOH, CP, FGG, F2, C1R, C4A/C4B, ITIH2, ITIH4, SERPINA1, FGB, AGT, HPX, C3, C1S, AHS, SERPINF1, C5, PLG, ALB, APOA1, TF, ORM1, C4BPA, ORM2, HRG, FGA, A2M
LXR/RXR activation	2.33E+01	4.80	KNG1, APOE, HPX, C3, APOB, APOH, AHS, SERPINF1, A1BG, C4A/C4B, ALB, APOA1, TF, ORM1, ITIH4, APOC1, ORM2, SERPINA1, PLTP, GC, FGA, APOD, AGT
FXR/RXR activation	2.28E+01	NaN	KNG1, APOE, HPX, C3, APOB, APOH, AHS, SERPINF1, A1BG, C4A/C4B, ALB, APOA1, TF, ORM1, ITIH4, APOC1, ORM2, SERPINA1, PLTP, GC, FGA, APOD, AGT
Complement system	1.91E+01	0.33	SERPINF1, C3, C1S, C8A, C5, C1R, C4A/C4B, C4BPA, CFIC7, C8B, C6, CFH, C8G
ILK signaling	1.19E+01	-2.67	ITGB1, MYH10, PARVA, MYH9, FEBLIM1, LIMS2, FERMT2, ILK, VIM, MYH11, MYL9, TGFB3, ITGA2, FLNA, ACTN4, VCL, ACTN1
Clathrin-mediated endocytosis signaling	1.19E+01	NaN	ITGB1, APOE, RAB5C, APOB, AP2B1, F2, ALB, APOA1, ACTA2, TF, ORM1, ARPC2, APOC1, ORM2, SERPINA1, ARPC4, APOD
Actin cytoskeleton signaling	9.80E+00	-3.21	ITGB1, KNG1, MYH10, MYH9, TLN1, MYLK, MYH11, F2, MYL9, ACTA2, FLNA, ARPC2, ACTN4, VCL, ACTN1, ARPC4
Coagulation system	9.10E+00	0.71	PLG, KNG1, FGB, SERPINA1, FGA, A2M, F2, FGG
Epithelial adherens junction signaling	9.06E+00	NaN	MYH10, MYH9, TUBA4A, MYH11, RAPIA, MYL9, ACTA2, SORBS1, ARPC2, VCL, ACTN4, ACTN1, ARPC4
Integrin signaling	8.31E+00	-3.74	ITGB1, PARVA, ILK, TLN1, MYLK, RAPIA, MYL9, ACTA2, ARPC2, ITGA1, ACTN4, VCL, ACTN1, ARPC4
Remodeling of epithelial adherens junctions	6.72E+00	NaN	RAB5C, ACTA2, ARPC2, TUBA4A, ACTN4, VCL, ARPC4, ACTN1
Atherosclerosis signaling	6.68E+00	NaN	APOE, ALB, APOA1, APOB, ORM1, APOC1, ORM2, SERPINA1, COL18A1, APOD

NaN not available

*z-score: predicted upregulation (positive) or downregulation (negative)

Table 2 Top 10 upstream regulators extracted using Ingenuity Pathway Analysis (IPA)

Upstream regulator (gene symbol)	Predicted activation state	p-value of overlap	Target molecules in dataset
<i>Tp53</i>	Transcription regulator	1.02E-26	A2M, ACTA2, ACTN1, ACTN4, ANXA6, APOA1, APOE, CNN1, COL14A1, COL18A1, COL6A2, CP, CSRPI, CTSSB, DSTN, EMILIN1, FERMT2, GC, HSP90AA1, HSPB1, HSPG2, IGFBP7, ILK, LAMA5, LASP1, LPP, LTBPI, MAP4, MCAM, MVP, MYH10, MYH9, MYL9, MYOF, PARVA, PDIA6, PGLYRP2, PLTP, SORBS1, SPP1, TGFB3, THBS1, TINAGL1, VCAN, VCL, VIM, VCAN, VCL, VIM, VCAN, VCL, VIM
<i>SRF</i>	Inhibited	9.28E-15	ACTA2, CALD1, CNN1, CSRPI, DSTN, FLNA, ITGA1, ITGB1, LMOD1, LMOD2, LMOD3, MYH11, MYL9, MYLK, PDLIM7, TAGLN, TNC, VCL
<i>MYOCD</i>	Inhibited	1.40E-10	ACTA2, CALD1, CNN1, GJA1, LMOD1, MYH11, MYLK, S100A4, TAGLN, TPM1
<i>TGFB1</i>	Inhibited	2.07E-10	ACTA2, ALB, CD44, CRIP2, FBLN5, HSPB1, IGFBP7, ITGA1, ITGB1, LAMC1, MFAP4, S100A4, SERPINA1, SOD3, SPP1, TAGLN, THBS1, TNC, VIM, YBX1
<i>HNF1A</i>	Activated	1.06E-09	AHS, ALB, ANPEP, ANXA4, APOH, C1S, C4BPA, C5, C8A, C8B, C8G, GC, ITIH4, SERPINA1, SERPING1
<i>Lh</i>	Activated	2.12E-09	ACTA2, ACTN1, ARPC4, COL15A1, COL18A1, GJA1, ILK, NPC2, RAB5C, THBS1, TLN1, TPM1, TPM2, VCL
<i>TNF</i>	Activated	2.72E-09	AEBP1, AGT, ALB, AOC3, APOE, C3, C5, CD44, CNN1, CP, CTSSB, DCN, GRN, HAPLN1, HSPG2, ITGB1, MCAM, MYLK, OGN, SOD3, TAGLN, TF, TNC, VCL, VIM
<i>MKLI</i>	Inhibited	4.92E-09	ACTA2, CNN1, FLNA, ITGB1, MYH11, MYH9, MYL9, TAGLN, TNC, VCL
<i>MYC</i>	Transcription regulator	6.95E-09	ACAN, ANXA4, ANXA6, CD44, COL14A1, COL15A1, COL18A1, COL6A3, FMOD, GDI1, GJA1, GLS, GLUD1, GPI, HAPLN1, ITGB1, LGALS1, MYL9, PDLIM7, THBS1, TNC

Discussion

Studies on atherosclerosis usually focus on specific well-known atherogenic molecular pathways, missing other key “unknown” pathways. In this study, we measured the human carotid atheroma proteome using mass spectrometry to identify differentially expressed proteins between paired early and advanced atherosclerotic lesions, which were analyzed for associated molecular functions and networks.

Atherosclerosis is a silent disease that can be detected after its initiation. In fact, most treatments for atherosclerosis focus on inhibiting lesion progression and maintaining plaque stability. Several proteomic studies have been conducted to identify protein biomarkers and molecular networks in atherosclerosis. These studies were mainly performed to identify biomarkers in the atherosclerotic secretome using *ex vivo* tissue models [5, 17], to identify abundant protein biomarkers in atherosclerotic lesions [18], or to identify molecular networks involved in carotid and aortic lesions in comparison to normal mammary or coronary arteries [19]. To our knowledge, this is the first study that compares advanced to early lesions. To identify proteins involved in atherosclerotic plaque progression, we compared the proteomes of paired samples obtained from advanced and early atherosclerotic lesions [20], which reduces the clinical and demographic variabilities among individuals and increases the statistical power of differential gene expression.

A total of 212 proteins were differentially expressed between advanced plaques and early lesions, clearly differentiating between the two tissue types. Interestingly, our data showed that downregulated proteins in advanced atherosclerotic lesions were mostly ECM components and cytoskeletal proteins related to the VSMC phenotype, in accordance with transcriptomic data analysis from other groups [21]. This finding suggests that these structural proteins are most likely deregulated at the transcriptional level in atherosclerotic plaque. This finding was also in line with previous studies showing major downregulations in proteins involved in VSMC differentiation and plaque stability in core plaques, compared to distal plaque regions [22] or mammary artery [17]. Of interest, our results showed that SRF and JUN, involved in VSMC development and phenotype regulation [23, 24], have enriched binding sites in the promoters of genes commonly downregulated at the mRNA and protein levels. In addition, the reduction in ECM proteins could be explained by the concomitant increase in the expression of proteases in advanced atherosclerotic lesions [25]. Indeed, recent studies have observed abundant expression of a set of metalloproteases and collagenases in carotid atheroma [17–19], concomitant with a reduction in collagen in symptomatic lesions [26]. In fact, proteolysis leads to ECM degradation fragments,

which cause an increase in the local immune response by inducing macrophage activation [27]. In addition, ChIP enrichment analysis (CHEA) indicates that NR1H3 is associated with upregulated genes/proteins related to complement activation in atherosclerotic foam cells. In line with this result, macrophages were previously shown to differentially express various complement-related genes [28], which suggests an involvement of NR1H3 in complement gene regulation.

Bioinformatics analysis identified RXR as overactivated in advanced compared to early lesions. This finding is in accordance with Hao et al., who previously reported that the RXR pathway was enriched in atherosclerotic lesions [18]. LXR transcriptional activity was shown to be induced in various modified forms of cholesterol and during macrophage differentiation [29] but also protects foam cells from apoptosis, thus promoting atheroma progression [30]. In contrast, several studies showed that RXR agonists exert atheroprotective effects [31, 32]. Nonetheless, our analysis indicates that RXR activation is usually associated with heterodimer formation with LXR and FXR. In fact, LXR α knockout in mice dramatically increased LDL and decreased HDL cholesterol levels in plasma [33]. Thus, the atheroprotective effects related to RXR activation could be due to systemic effects on body cholesterol levels and mediated only during early stages of atherosclerotic lesions.

Deficiency in p53 was shown to accelerate atherosclerotic plaque development through cell-specific effects via the regulation of cellular proliferation and apoptosis in endothelial cells (ECs), macrophages, and VSMCs [34]. In both ApoE^{-/-} and LDL receptor^{-/-} mice, macrophage-specific p53 deficiency enhanced atherosclerotic lesion development and vulnerability, mainly through decreased macrophage apoptosis or increased macrophage proliferation [35, 36]. Similarly, p53 also induces endothelial apoptosis under oxidative stress conditions. However, the role of p53 in VSMC apoptosis is controversial. Induction of p53 inhibits neointima formation [37] and increases advanced plaque instability, probably by inducing cap VSMC apoptosis and their transition from a synthetic to a contractile phenotype [38, 39]. However, endogenous p53 in VSMCs was not found to be proapoptotic or growth suppressive [38]; rather, it may reduce atherosclerosis by reducing VSMC apoptosis [40]. Nevertheless, our results indicate that VSMC apoptosis could be induced by other mechanisms, such as the inhibition of ILK signaling [41], which may also lead to endothelial [42] and VSMC [43] dysfunctions. Therefore, our results suggest no significant global change in p53 expression during atheroma progression, which could be due to a balance in its expression levels in different atherosclerotic cells.

p53 inhibition, along with shear stress and oxidized LDL, may enhance the expression of c-myc [44–46], a

transcription factor that regulates the expression of various genes involved in cellular metabolism, growth, proliferation, and apoptosis. In fact, c-myc was shown to be expressed in early atherosclerotic lesions [47], mainly in VSMCs [48]. C-myc was also demonstrated to enhance atherosclerotic lesion progression through the induction of VSMC proliferation [49], macrophage activation [50] and ECM remodeling [46].

TGFB1 was among the most connected proteins in the molecular network, in addition to other well-known proatherogenic proteins, such as TNF, ERK, JNK, ERK1, and MAPK. Little is known about the role of TGFb1, which mainly performs atheroprotective functions [51]. Our results suggest that TGFb is downregulated during atheroma progression, but is also highly connected with other deregulated proteins, which raises the importance of this protein for further molecular analysis.

Of interest, the 4 transcription factors LRRFIP1, FBLIM1, CRIP2, and FHL3 were downregulated in advanced compared to early lesions. The leucine-rich repeat in FLII interacting protein 1 (LRRFIP1) was previously shown to induce VSMC proliferation and to regulate platelet function [52, 53]. Even though VSMC proliferation is known to aggravate atherosclerotic plaque development during early stages, it plays a beneficial role in advanced plaque stability by providing a physical support for the fibrous cap. In accordance with our data, loss of Cysteine-Rich Protein 2 (CRIP2), involved in VSMC development and maintenance, was shown to induce atherosclerotic plaque progression and susceptibility to rupture [54].

Except for angiotensinogen (AGT) and APOC1, none of the top 10 upregulated and downregulated proteins were previously described in atherosclerosis. AGT is the substrate for the renin-angiotensin aldosterone system (RAAS), which is known to play major roles in atherosclerotic plaque initiation and progression [55]. Previous studies have suggested that AGT expression is influenced by several atherogenic factors, including vascular injury, increased sodium diet, insulin resistance, and high cortisol levels [56]. Similarly, APOC1, also upregulated in advanced lesions, was shown to aggravate atherosclerosis under inflammatory conditions [57].

In conclusion, our study revealed 95 upregulated and 117 downregulated proteins in advanced compared to early atherosclerotic lesions. The downregulated proteins are mainly related to tissue remodeling, whereas the upregulated proteins are mainly associated with proinflammatory response. Our study is mainly focused on the identification of candidate pathways and upstream regulators that are involved in atherosclerotic lesion development. The main regulators identified were not altered at the protein level, which points to posttranslational modifications. A more focused and thorough analysis of such modifications is

needed in future studies. In addition, our study raises questions about the clinical interpretations of cell-specific gene modulation in vitro and in animal models. Finally, our study raises the importance of certain pathways and reveals new proteins and transcription factors that could have central roles in atherosclerotic lesion progression.

Funding A.N. was awarded a scholarship from “La Nouvelle Société Francophone d’Athérosclérose” (NSFA). This work was supported by a Campus France grant from “Coopération pour l’Évaluation et le Développement de la Recherche” (CEDRE).

Compliance with ethical standards

Conflict of interest The authors declare that they have no conflict of interest.

Publisher’s note: Springer Nature remains neutral with regard to jurisdictional claims in published maps and institutional affiliations.

References

1. WHO | The top 10 causes of death. WHO. <http://www.who.int/mediacentre/factsheets/fs310/en/index.html>. Accessed 27 Feb 2013.
2. Vinereanu D. Risk factors for atherosclerotic disease: present and future. *Herz*. 2006;31 (Suppl 3):5–24.
3. Libby P. Inflammation and cardiovascular disease mechanisms. *Am J Clin Nutr*. 2006;83:456S–460S.
4. Sakakura K, Nakano M, Otsuka F, Ladich E, Kolodgie FD, Virmani R. Pathophysiology of atherosclerosis plaque progression. *Heart Lung Circ*. 2013;22:399–411. <https://doi.org/10.1016/j.hlc.2013.03.001>
5. Vivanco F, Padiál LR, Darde VM, de la Cuesta F, Alvarez-Llamas G, Diaz-Prieto N, et al. Proteomic biomarkers of atherosclerosis. *Biomark Insights*. 2008;3:101–13.
6. World Medical Association declaration of Helsinki. Recommendations guiding physicians in biomedical research involving human subjects. *JAMA*. 1997;277:925–6.
7. Sary HC. Natural history and histological classification of atherosclerotic lesions: an update. *Arterioscler Thromb Vasc Biol*. 2000;20:1177–8.
8. Tsai T-H, Song E, Zhu R, Di Poto C, Wang M, Luo Y, et al. LC-MS/MS-based serum proteomics for identification of candidate biomarkers for hepatocellular carcinoma. *Proteomics*. 2015;15:2369–81. <https://doi.org/10.1002/pmic.201400364>
9. Blagoev B, Ong S-E, Kratchmarova I, Mann M. Temporal analysis of phosphotyrosine-dependent signaling networks by quantitative proteomics. *Nat Biotechnol*. 2004;22:1139–45. <https://doi.org/10.1038/nbt1005>
10. Heberle H, Meirelles GV, da Silva FR, Telles GP, Minghim R. InteractiVenn: a web-based tool for the analysis of sets through Venn diagrams. *BMC Bioinform*. 2015;16. <https://doi.org/10.1186/s12859-015-0611-3>
11. Ringnér M. What is principal component analysis? *Nat Biotechnol*. 2008;26:303–4. <https://doi.org/10.1038/nbt0308-303>
12. Mi H, Poudel S, Muruganujan A, Casagrande JT, Thomas PD. PANTHER version 10: expanded protein families and functions, and analysis tools. *Nucleic Acids Res*. 2016;44:D336–342. <https://doi.org/10.1093/nar/gkv1194>
13. Kuleshov MV, Jones MR, Rouillard AD, Fernandez NF, Duan Q, Wang Z, et al. Enrichr: a comprehensive gene set enrichment

- analysis web server 2016 update. *Nucleic Acids Res.* (e-pub ahead of print 3 May 2016; <https://doi.org/10.1093/nar/gkw377>).
14. Bonnet A, Lagarrigue S, Liaubet L, Robert-Granié C, SanCristobal M, Tosser-Klopp G. Pathway results from the chicken data set using GOTM, Pathway Studio and Ingenuity softwares. *BMC Proc.* 2009;3:S11 <https://doi.org/10.1186/1753-6561-3-S4-S11>
 15. Yuryev A, Kotelnikova E, Daraselia N. Ariadne's ChemEffect and Pathway Studio knowledge base. *Expert Opin Drug Discov.* 2009;4:1307–18. <https://doi.org/10.1517/17460440903413488>
 16. Krämer A, Green J, Pollard J, Tugendreich S. Causal analysis approaches in Ingenuity Pathway Analysis. *Bioinforma Oxf Engl.* 2014;30:523–30. <https://doi.org/10.1093/bioinformatics/btt703>
 17. Aragonès G, Auguet T, Guiu-Jurado E, Berlanga A, Curriu M, Martínez S, et al. Proteomic profile of unstable atheroma plaque: increased neutrophil defensin 1, clusterin, and apolipoprotein E levels in carotid secretome. *J Proteome Res.* 2016;15:933–44. <https://doi.org/10.1021/acs.jproteome.5b00936>
 18. Hao P, Ren Y, Pasterkamp G, Moll FL, de Kleijn DPV, Sze SK. Deep proteomic profiling of human carotid atherosclerotic plaques using multidimensional LC-MS/MS. *Proteom Clin Appl.* 2014;8:631–5. <https://doi.org/10.1002/prca.201400007>
 19. Herrington DM, Mao C, Parker SJ, Fu Z, Yu G, Chen L, et al. Proteomic architecture of human coronary and aortic atherosclerosis. *Circulation.* 2018;137:2741–56. <https://doi.org/10.1161/CIRCULATIONAHA.118.034365>
 20. Bricca G, Legedz L, Nehme A, Ayari H, ne Paultre C, Hodroj W, et al. Local angiotensin pathways in human carotid atheroma: towards a systems biology approach, local angiotensin pathways in human carotid atheroma: towards a systems biology approach. *Conf Pap Sci Conf Pap Sci.* 2015;2015:e593086. <https://doi.org/10.1155/2015/593086>
 21. Cagnin S, Biscuola M, Patuzzo C, Trabetti E, Pasquali A, Laveder P, et al. Reconstruction and functional analysis of altered molecular pathways in human atherosclerotic arteries. *BMC Genom.* 2009;10:13 <https://doi.org/10.1186/1471-2164-10-13>
 22. Rocchiccioli S, Pelosi G, Rosini S, Marconi M, Viglione F, Citti L, et al. Secreted proteins from carotid endarterectomy: an untargeted approach to disclose molecular clues of plaque progression. *J Transl Med.* 2013;11:260 <https://doi.org/10.1186/1479-5876-11-260>
 23. Camoretti-Mercado B, Dulin NO, Solway J. SRF function in vascular smooth muscle when less is more? *Circ Res.* 2005;97:409–10. <https://doi.org/10.1161/01.RES.0000181546.77857.7f>
 24. Ohtsu H, Mifune M, Frank GD, Saito S, Inagami T, Kim-Mitsuyama S, et al. Signal-crosstalk between Rho/ROCK and c-Jun NH2-terminal kinase mediates migration of vascular smooth muscle cells stimulated by angiotensin II. *Arterioscler Thromb Vasc Biol.* 2005;25:1831–6. <https://doi.org/10.1161/01.ATV.0000175749.41799.9b>
 25. Garcia-Touchard A, Henry TD, Sangiorgi G, Spagnoli LG, Mauriello A, Conover C, et al. Extracellular proteases in atherosclerosis and restenosis. *Arterioscler Thromb Vasc Biol.* 2005;25:1119–27. <https://doi.org/10.1161/01.ATV.0000164311.48592.da>
 26. Langley SR, Willeit K, Didangelos A, Matic LP, Skrobilin P, Barallobre-Barreiro J, et al. Extracellular matrix proteomics identifies molecular signature of symptomatic carotid plaques. *J Clin Invest.* 2017;127:1546–60. <https://doi.org/10.1172/JCI86924>
 27. Adair-Kirk TL, Senior RM. Fragments of extracellular matrix as mediators of inflammation. *Int J Biochem Cell Biol.* 2008;40:1101–10. <https://doi.org/10.1016/j.biocel.2007.12.005>
 28. Luo C, Chen M, Madden A, Xu H. Expression of complement components and regulators by different subtypes of bone marrow-derived macrophages. *Inflammation.* 2012;35:1448–61. <https://doi.org/10.1007/s10753-012-9458-1>
 29. A-González N, Castrillo A. Liver X receptors as regulators of macrophage inflammatory and metabolic pathways. *Biochim Biophys Acta.* 2011;1812:982–94. <https://doi.org/10.1016/j.bba-dis.2010.12.015>
 30. Hamada M, Nakamura M, Tran MTN, Moriguchi T, Hong C, Ohsumi T, et al. MafB promotes atherosclerosis by inhibiting foam-cell apoptosis. *Nat Commun.* 2014;5:3147 <https://doi.org/10.1038/ncomms4147>
 31. Claudel T, Leibowitz MD, Fiévet C, Tailleux A, Wagner B, Repa JJ, et al. Reduction of atherosclerosis in apolipoprotein E knockout mice by activation of the retinoid X receptor. *Proc Natl Acad Sci USA.* 2001;98:2610–5. <https://doi.org/10.1073/pnas.041609298>
 32. Lalloyer F, Fiévet C, Lestavel S, Torpier G, van der Veen J, Touche V, et al. The RXR agonist bexarotene improves cholesterol homeostasis and inhibits atherosclerosis progression in a mouse model of mixed dyslipidemia. *Arterioscler Thromb Vasc Biol.* 2006;26:2731–7. <https://doi.org/10.1161/01.ATV.0000248101.93488.84>
 33. Bradley MN, Hong C, Chen M, Joseph SB, Wilpitz DC, Wang X, et al. Ligand activation of LXR beta reverses atherosclerosis and cellular cholesterol overload in mice lacking LXR alpha and apoE. *J Clin Invest.* 2007;117:2337–46. <https://doi.org/10.1172/JCI31909>
 34. Mercer J, Bennett M. The role of p53 in atherosclerosis. *Cell Cycle Georget Tex.* 2006;5:1907–9. <https://doi.org/10.4161/cc.5.17.3166>
 35. Guevara NV, Kim HS, Antonova EI, Chan L. The absence of p53 accelerates atherosclerosis by increasing cell proliferation in vivo. *Nat Med.* 1999;5:335–9. <https://doi.org/10.1038/6585>
 36. Merched AJ, Williams E, Chan L. Macrophage-specific p53 expression plays a crucial role in atherosclerosis development and plaque remodeling. *Arterioscler Thromb Vasc Biol.* 2003;23:1608–14. <https://doi.org/10.1161/01.ATV.0000084825.88022.53>
 37. George SJ, Angelini GD, Capogrossi MC, Baker AH. Wild-type p53 gene transfer inhibits neointima formation in human saphenous vein by modulation of smooth muscle cell migration and induction of apoptosis. *Gene Ther.* 2001;8:668–76. <https://doi.org/10.1038/sj.gt.3301431>
 38. Bennett MR, Littlewood TD, Schwartz SM, Weissberg PL. Increased sensitivity of human vascular smooth muscle cells from atherosclerotic plaques to p53-mediated apoptosis. *Circ Res.* 1997;81:591–9.
 39. von der Thüsen JH, van Vlijmen BJM, Hoeben RC, Kockx MM, Havekes LM, van Berkel TJC, et al. Induction of atherosclerotic plaque rupture in apolipoprotein E^{-/-} mice after adenovirus-mediated transfer of p53. *Circulation.* 2002;105:2064–70.
 40. Mercer J, Figg N, Stoneman V, Braganza D, Bennett MR. Endogenous p53 protects vascular smooth muscle cells from apoptosis and reduces atherosclerosis in ApoE knockout mice. *Circ Res.* 2005;96:667–74. <https://doi.org/10.1161/01.RES.0000161069.15577.ca>
 41. Abboud ER, Coffelt SB, Figueroa YG, Zvezdaryk KJ, Nelson AB, Sullivan DE, et al. Integrin-linked kinase: a hypoxia-induced anti-apoptotic factor exploited by cancer cells. *Int J Oncol.* 2007;30:113–22.
 42. Herranz B, Marquez S, Guijarro B, Aracil E, Aicart-Ramos C, Rodriguez-Crespo I, et al. Integrin-linked kinase regulates vasomotor function by preventing endothelial nitric oxide synthase uncoupling: role in atherosclerosis. *Circ Res.* 2012;110:439–49. <https://doi.org/10.1161/CIRCRESAHA.111.253948>
 43. Ho B, Bendeck MP. Integrin linked kinase (ILK) expression and function in vascular smooth muscle cells. *Cell Adhes Migr.* 2009;3:174–6.

44. Sachdeva M, Zhu S, Wu F, Wu H, Walia V, Kumar S, et al. p53 represses c-Myc through induction of the tumor suppressor miR-145. *Proc Natl Acad Sci USA*. 2009;106:3207–12. <https://doi.org/10.1073/pnas.0808042106>
45. de Nigris F, Youssef T, Ciafré S, Franconi F, Anania V, Condorelli G, et al. Evidence for oxidative activation of c-Myc-dependent nuclear signaling in human coronary smooth muscle cells and in early lesions of Watanabe heritable hyperlipidemic rabbits: protective effects of vitamin E. *Circulation*. 2000;102:2111–7.
46. Magid R, Murphy TJ, Galis ZS. Expression of matrix metalloproteinase-9 in endothelial cells is differentially regulated by shear stress. Role of c-Myc. *J Biol Chem*. 2003;278:32994–9. <https://doi.org/10.1074/jbc.M304799200>
47. Toutouzas K, Messaris E, Konstadoulakis M, Chatzigianni E, Karayannis M, Davaris P, et al. Expression of c-myc and H-ras and Absence of Expression of p53 and bcl-2 Genes in Atherosclerotic Human Carotid Arteries - 1297.pdf. *J Clin Basic Cardiol*. 2002;5:253–6.
48. Marin ML, Gordon RE, Veith FJ, Tulchin N, Panetta TF. Distribution of c-myc oncoprotein in healthy and atherosclerotic human carotid arteries. *J Vasc Surg*. 1993;18:170–6. discussion176-177
49. Díez J, Panizo A, Hernández M, Galindo MF, Cenarruzabeitia E, Pardo Mindán FJ. Quinapril inhibits c-Myc expression and normalizes smooth muscle cell proliferation in spontaneously hypertensive rats. *Am J Hypertens*. 1997;10:1147–52.
50. Pello OM, De Pizzol M, Mirolo M, Soucek L, Zammataro L, Amabile A, et al. Role of c-MYC in alternative activation of human macrophages and tumor-associated macrophage biology. *Blood*. 2012;119:411–21. <https://doi.org/10.1182/blood-2011-02-339911>
51. Grainger DJ. Transforming growth factor beta and atherosclerosis: so far, so good for the protective cytokine hypothesis. *Arterioscler Thromb Vasc Biol*. 2004;24:399–404. <https://doi.org/10.1161/01.ATV.0000114567.76772.33>
52. Goodall AH, Burns P, Salles I, Macaulay IC, Jones CI, Ardissino D, et al. Bloodomics Consortium Transcription profiling in human platelets reveals LRRFIP1 as a novel protein regulating platelet function. *Blood*. 2010;116:4646–56. <https://doi.org/10.1182/blood-2010-04-280925>.
53. Choe N, Kwon J-S, Kim J-R, Eom GH, Kim Y, Nam K-I, et al. The microRNA miR-132 targets Lrrfip1 to block vascular smooth muscle cell proliferation and neointimal hyperplasia. *Atherosclerosis*. 2013;229:348–55. <https://doi.org/10.1016/j.atherosclerosis.2013.05.009>
54. Wei J, Gorman TE, Liu X, Ith B, Tseng A, Chen Z, et al. Increased neointima formation in cysteine-rich protein 2-deficient mice in response to vascular injury. *Circ Res*. 2005;97:1323–31. <https://doi.org/10.1161/01.RES.0000194331.76925.5c>
55. Durante A, Peretto G, Laricchia A, Ancona F, Spartera M, Mangieri A, et al. Role of the renin-angiotensin-aldosterone system in the pathogenesis of atherosclerosis. *Curr Pharm Des*. 2012;18:981–1004.
56. Bricca G, Legedz L, Nehme A, Ayari H, Paultre C, Hodroj W, et al. Local angiotensin pathways in human carotid atheroma: towards a systems biology approach. *Conf Pap Sci*. 2015;2015. <https://doi.org/10.1155/2015/593086>
57. Westertep M, Berbée JFP, Pires NMM, van Mierlo GJD, Kleemann R, Romijn JA, et al. Apolipoprotein C-II is crucially involved in lipopolysaccharide-induced atherosclerosis development in apolipoprotein E-knockout mice. *Circulation*. 2007;116:2173–81. <https://doi.org/10.1161/CIRCULATIONAHA.107.693382>.